Hindawi
Geofluids
Volume 2021, Article ID 3691549, 12 pages
https://doi.org/10.1155/2021/3691549

Research Article

Effects of Oil Contamination on the Physical-Mechanical Behavior of Loess and Its Mechanism Analysis

Shibin Zhang,[1] **Rongjian Li**,[1,2] **Weishi Bai**,[1] **and Qiang Yang**[1,3]

[1]*Institute of Geotechnical Engineering, Xi'an University of Technology, Xi'an 710048, China*
[2]*Shaanxi Key Laboratory of Loess Mechanics and Engineering, Xi'an University of Technology, Xi'an 710048, China*
[3]*Center for Hydrogeology and Environmental Geology, CGS, Baoding 0711051, China*

Correspondence should be addressed to Rongjian Li; lirongjian@xaut.edu.cn

Received 22 October 2021; Revised 16 November 2021; Accepted 24 November 2021; Published 7 December 2021

Academic Editor: Peng Hou

Oil leakage will not only pollute the soil but also change its physical-mechanical behavior, and loess has complex properties in the environment of oil presence. Artificial loess contaminated by diesel oil is collected as the research object. The physical and mechanical properties of clean loess and contaminated loess, including liquid and plastic limits, permeability, compression properties, and compressive strength characteristics, are estimated through a series of laboratory tests under different oil contents, water contents, and dry densities. Results show that liquid limits, plastic limits, and permeability coefficient of diesel-contaminated loess decrease with the increase of oil content. The compression modulus and compressive strength of diesel-contaminated loess increase with the increase of dry density at the same oil content. Adding diesel oil, the change law of the unconfined compressive strength of contaminated loess is opposite at the two different water contents. The variation of the compression modulus and unconfined compressive strength of diesel oil-contaminated loess is basically identical at the same condition. The findings of this study would be expected to bridge the gap between theory and practice in treatment and remediation of contaminated soil in the region of oil production.

1. Introduction

Oil leakage is accidental in most cases, such as oil exploitation, transportation pipeline damage, coastal facility discharge, and oil tank accident. The cases of soil and water contaminated by oil leakage are increasingly serious [1, 2]. Oil leakage causes frequent pollution events to soil and environment, which is a serious problem worldwide [3]. Oil leakage not only contaminates the soil but also changes its physical and mechanical properties [4–6].

The largest oil contamination was caused by the Kuwait Gulf War in history, making large-scale water and land seriously contaminated by crude oil [7], and the problem of soil contaminated by oil leakage is increasingly concerned by scholars. Alsanad et al. [8, 9] performed a series of tests considering the aging of oil, studied the effects of crude oil on the physical and mechanical properties of Kuwaiti sand, and found that the physical and mechanical properties of oil-contaminated Kuwaiti sand would be affected by oil content and the aging of oil. Nasr [10] carried out laboratory tests to evaluate the effect of oil content on the bearing capacity characteristics of oil-contaminated sand and the settlement of the footing and found that the load settlement characteristics and ultimate bearing capacity of footing could be significantly decreased by oil pollution. Chaplin et al. [11] studied the strength, compression, and permeability characteristics of crude oil-contaminated sand and obtained a decrease in strength and permeability and an increase in the compressibility of contaminated sand with the increase of oil content. Aiban [12] concluded that the water content and temperature had a certain effect on the physical and mechanical properties of oil-contaminated sand. Al-Aghbari et al. [13] showed a decrease in optimal water content, permeability, internal friction angle, and strength of sand contaminated by oil. Abousnina et al. [14] studied the physical and mechanical properties of contaminated fine sand and concluded that the water absorption, permeability, and shear strength of sand decreased with the

increase of oil content. Ostovar et al. [15] carried out a series of laboratory tests to study the effect of crude oil contamination on properties of permeability and bearing capacity. Fazeli et al. [16] studied the strength and bearing capacity characteristics of the oil-contaminated sand through the direct shear tests and bearing capacity tests of strip shallow foundation, and the results showed that oil content had an important effect on the shear strength and bearing capacity characteristics of sand. In the abovementioned studies, the physical-mechanical behaviors of sand contaminated by oil are basically the same.

However, researchers also evaluate the physical-mechanical behaviors of other types of oil-contaminated soil. Khamehchiyan et al. [17] studied the geotechnical properties of sand and clay polluted by crude oil. Rahman et al. [18] prepared oil-contaminated soil samples by mixing air-dried residual soil and oil and carried out laboratory tests. They found that oil pollution led to deterioration of the geotechnical properties of soil samples, and compared with clean residual soil, their maximum dry density, optimal water content, permeability, and shear strength reduced. Zheng et al. [19, 20] studied the physical and mechanical properties of diesel oil-contaminated silty clay by mixing air-dried silty clay with different amounts of oil. They reported that the maximum dry density, optimum water content, and permeability of samples decreased with the increase of the pollution degree; meanwhile, the change of unconfined compressive strength was related to the oil content and water content of the samples. Safehian et al. [21] prepared contaminated soil samples by mixing dried clay and diesel oil, carried out a series of laboratory tests, and found that the physical-mechanical behaviors of clay were relatively complex under diesel pollution. Khosravi et al. [22] conducted a series of laboratory tests on the preparation of contaminated kaolin samples by mixing dried kaolin with gasoline. They observed that there is a decrease in the internal friction angle of gasoline-contaminated kaolin samples, the cohesion increased, and the shear strength slightly changed. Xie et al. [23] and Li et al. [24] performed an unconfined compressive strength test to study the strength and deformation characteristics of oil-polluted coastal saline soil samples by mixing oil with coastal saline soil of known water content. Iqbal et al. [25] carried out a series of laboratory tests to study the permeability and mechanical properties of low plastic soil. Based on the abovementioned studies, the physical-mechanical behaviors are relatively complex for different types of soil, such as fine-grained soil, clay, and kaolin soil.

Oil spills have polluted loess in the region of loess oil production, which always occurs. However, in the study of different types of soil contaminated by oil, little information is available for dealing with the evaluation of the physical-mechanical behavior of oil-contaminated loess. As a typical organic polluted soil, oil leakage pollution is bound to have a certain impact on the physical-mechanical properties of loess. Therefore, evaluating the physical-mechanical behavior of oil-contaminated loess is necessary under different laboratory test conditions.

2. Scope of the Problem

The northern Shaanxi region of China is rich in petroleum resources and is an important energy base. However, its ecological environment is very fragile and soil erosion is serious. In addition, in recent years, with the expansion of the oil exploitation scale and backward exploitation technology, the pollution caused by resource exploration and development to the ecological environment of the whole region is becoming increasingly serious. Loess is the main soil type in this region, and it is widely distributed. In the region of oil production, the environmental problems caused by oil exploration, exploitation, transportation, and storage need to be solved urgently. The pollution of loess caused by crude oil leakage has always been a widely concerned problem. Based on the research of oil pollution prevention and control technology in the region of loess oil production, the physical-mechanical behavior of oil-contaminated loess is carried out to understand the impact of oil pollution on the properties of loess. This study provides technical support for further research on the bearing capacity and effective remediation of oil-contaminated sites in the region of the loess oil production and provides a strong guarantee for more rational and effective development and utilization of land.

3. Experimental Procedure

3.1. Materials. In this study, pure loess was collected from the construction site of the slope engineering in the region of loess oil production of northern Shaanxi, and the depth of soil sample collection was 2.5–3.5 m. Loess was chosen as a typical type of unsaturated soil for laboratory tests, as shown in Figure 1(a). The properties of loess samples are relatively uniform, and its main physical parameters are as shown in Table 1.

Diesel oil collected from China Petrochemical Group was selected as a typical representative of petroleum oil, as seen in Figure 1(b). After the crude petroleum was leaked, its own viscosity determined the infiltration of crude petroleum in the same region. The greater the viscosity of oil, the weaker its ability to infiltrate the loess. The diesel oil is part of light nonaqueous phase liquids, its viscosity is far less than that of crude petroleum, and it has greater pollution potential. In addition, diesel oil accounts for a large proportion of the products refined from crude petroleum, which is a typical fuel oil fractionated. Diesel oil is also very difficult to volatilize in the testing environment; it is relatively safer to carry out a series of laboratory tests. In comparison with diesel oil, gasoline is very volatile at room temperature, which is more dangerous during the tests. Table 2 presents the basic parameters of diesel oil.

3.2. Methods. The process of loess polluted by oil might be long in nature, and it gradually reached a certain oil-bearing state in loess under the influence of various factors. Oil content refers to the percentage of diesel oil in unit mass loess, that is, the ratio of diesel oil quality to clean dry loess quality in oil-contaminated loess [26]. According to the

(a) Pure loess (b) Diesel oil

Figure 1: Experimental materials.

Table 1: Physical parameters of loess.

Soil sample	Natural water content (%)	Optimum water content (%)	Maximum dry density (g/cm^3)	Liquid limits (LL) (%)	Plastic limits (PL) (%)
Loess	12	19.6	1.69	32.2	11.7

Table 2: Physical parameters of diesel.

Oil sample	Density (g/cm^3)	Viscosity coefficient (mm^2/s)	Surface tension (mN/m)	Freezing point (°C)
Diesel oil	0.846	3.9	1.77	−20

research methods of relevant literatures [27–30], the value range of oil content of contaminated soil is 0-20% in literatures [21, 22]. The oil content of contaminated soil represents the degree of pollution. The oil content increases from 0 to 16%, which simulates the pollution degree of loess increases gradually. Therefore, the oil contents of contaminated loess ranged from 0 to 16% in this study, which was prepared by adding diesel oil with quantitative calculation to the pure loess with known water content. In order to study the influence of water content on the physical-mechanical behavior of oil-contaminated loess, two commonly used water contents of loess samples are considered in this manuscript. And 12% is the natural water content of loess samples, and 19.6% is optimum water content, which lays a foundation for the study of other properties of oil-contaminated loess.

According to GB/T 50123-2019 [31], Atterberg limits tests, permeability tests, compression tests, and unconfined compressive strength tests were used to study the physical and mechanical behaviors of clean and oil-contaminated loess. To avoid the effect of temperature on the test results, this test was conducted at room temperature of 20°C. The standards for the specimens' sizes of these tests were based on GB/T 50123-2019.

Atterberg limits tests were carried out on the clean and contaminated loess with different oil contents ($n = 0$, 2%, 4%, 8%, 12%, and 16%) by weight of dry loess. After 7 days of uniform aging of diesel-contaminated loess, each sample was prepared with different consistencies of soil paste for three tests, ensuring that the sinking depth of each sample is 4–5, 9–10, and 16–18 mm, respectively. Based on GB/T 50123-2019, the plastic limits and liquid limits of each oil-contaminated loess corresponded to 2 and 17 mm used as the water content, respectively. Permeability tests were conducted on the clean loess and diesel-contaminated loess with different oil contents ($n = 0$, 2%, 4%, 8%, 12%, and 16%) and dry densities ($\rho_d = 1.35$, 1.45, and 1.55 g/cm^3), and the specimen size was Φ61.8 mm × 40 mm.

According to GB/T 50123-2019, the specimen size of clean and contaminated loess was Φ79.8 mm × 20 mm under compression tests. A vertical stepwise loading method is adopted in compression tests, with the pressure range of 50, 100, 200, 400, and 800 kPa, and the deformation of the samples under each level of load is recorded. The unconfined compressive strength tests were conducted on loess specimens, and the specimen size was Φ39.1 mm × 80 mm. The coefficient of measuring ring was 1.0993 N/0.01 mm, and the shear rate was 0.368 mm/min. Then, the stress value was measured every 0.1 mm interval deformation, and the maximum axial stress was used as the unconfined compressive strength of diesel-contaminated loess. Compression tests and unconfined compressive strength tests were carried out on samples with different water contents (natural water content $w = 12\%$ and optimal water content $w = 19.6\%$), oil contents ($n = 0$, 2%, 4%, 8%, 12%, and 16%), and dry densities ($\rho_d = 1.35$, 1.45, and 1.55 g/cm^3).

3.3. Sample Preparation. Diesel-contaminated loess specimens were prepared by directly mixing diesel oil and pure loess, for the good fluidity of diesel oil. The prepared oil-

(a) Loess before contamination (b) Loess after contamination with 12% diesel oil

Figure 2: The loess before and after contamination with 12% diesel oil.

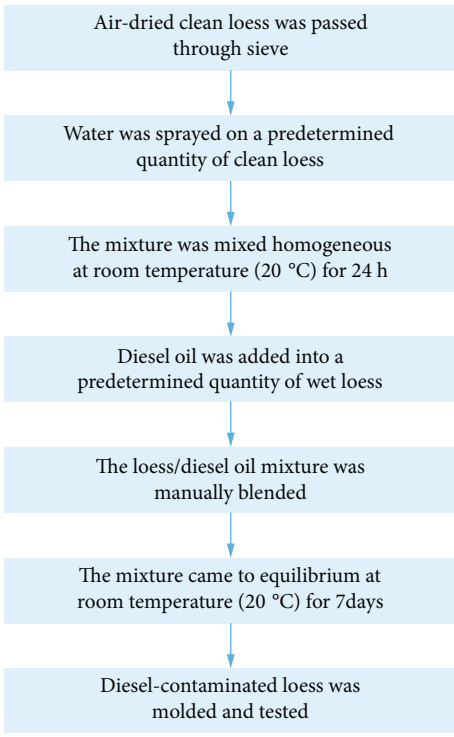

Figure 3: Sample preparation methods of oil-contaminated loess.

contaminated loess specimens were placed in a closed container for 7 days to make the oil and soil fully contact and mix evenly. During this period, the container should be turned upside down to prevent diesel oil from accumulating at the bottom under the action of gravity to form a specimen with uneven concentration. Figure 2 shows the loess before and after contamination with 12% diesel oil.

Notably, the sample preparation method was adopted in this study. As presented in Figure 3, the method of sample preparation was that air-dried clean loess was passed through a sieve of 2 mm. Two kinds of water content ($w = 12\%$, 19.6%) were prepared by adding distilled water to air-dried clean loess. After the loess samples stood for 24 h, quantitative diesel oil was added to prepare the contaminated samples with oil content (from 2% to 16%). Then, the oil-contaminated samples were placed in a closed container and stood for 7 days at room temperature of 20°C. During this period, the container was turned upside down to evenly mix the diesel oil and loess.

4. Results and Discussion

4.1. Liquid and Plastic Limits of Contaminated Loess. The primary physical state characteristic of loess is consistency, which refers to the soft and hard degree of loess or its resistance to deformation or damage caused by external forces. Atterberg limits or consistency of loess is characterized by liquid limits (LL), plastic limits (PL), and plasticity index (PI). Accurately measuring the water content of oil-contaminated porous media is important for the study of its physical, chemical, mechanical, and hydraulic properties [32]. Given the complexity of diesel oil in the pore fluid of contaminated loess, the conventional calculation equation is not suitable for the determination of the water content of diesel-contaminated loess. Thus, water content can be determined by the following equations:

$$w = \frac{m_{\mathrm{w}}}{m_{\mathrm{d}}}, \tag{1}$$

where w is the water content of diesel-contaminated loess, m_{d} is the mass of dried loess, and m_{w} is the mass of water, and $m_{\mathrm{w}} = (m_t - m_r) - m_0$, bringing it into Equation (1):

$$w = \frac{(m_t - m_r) - m_0}{m_{\mathrm{d}}}, \tag{2}$$

where m_t is the mass of wet contaminated loess, m_0 is the mass of other volatile substances except for water, m_r is the mass of diesel-contaminated loess after drying, and $m_r = m_{\mathrm{d}} + m_{\mathrm{d}} n\gamma$; then,

$$m_d = \frac{m_r}{1 + n\gamma}, \tag{3}$$

where n is the oil content of diesel-contaminated loess before drying and γ is the diesel oil residual content after drying.

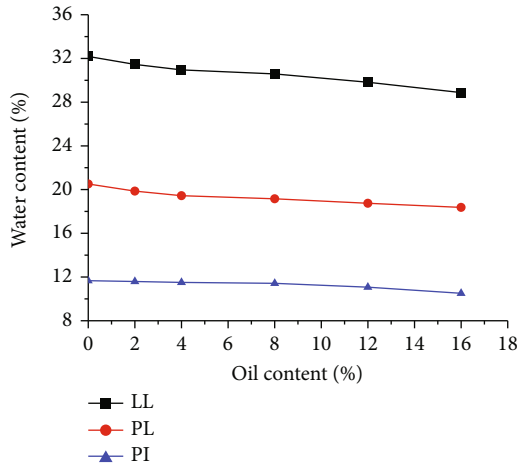

Figure 4: Variation curve of LL and PL of diesel-contaminated loess with different oil contents.

Equation (4) can be deduced by Equation (3) and $m_0 = m_d$ $n(1-\gamma)$:

$$m_0 = \frac{m_r n(1-\gamma)}{1+\gamma}. \quad (4)$$

Substituting Equations (3) and (4) into Equation (2):

$$w = \frac{m_t}{m_d}(1+n\gamma) - (1+n). \quad (5)$$

Therefore, Equation (5) is applied to determine the water content of diesel-contaminated loess specimens in all tests of this study.

The Atterberg limits of loess contaminated by different diesel oil contents are determined to evaluate the effects of contamination on the physical properties of the soil. Relationships between liquid and plastic limits of diesel-contaminated loess and oil content are presented in Figure 4.

As can be seen from Figure 4, liquid limits (LL), plastic limits (PL), and plasticity index (PI) decrease with the increase of oil content. The variation range of PL and LL of diesel-contaminated loess is 18.37%–20.51% and 28.88%–32.18%, respectively, as the oil content increases from 0 to 16%. In addition, the range of PI of diesel-contaminated loess is 10.51–11.67, which changes gentler than that of LL and PL.

The PI of loess indicates the range of water content when the loess is plastic. The higher the PI of loess, the more water can be absorbed [33]. A decrease in PI of loess contaminated by diesel is found in this research, which is in agreement with those studied by Khamehchiyan et al. [17] and Khosravi et al. [22], but it is inconsistent with the results of Kermani and Ebadi [34]. The presence of double-layer water causes the plasticity of loess. The innermost layer of double-layer adsorbed water is strongly held by soil. This orientation of the water surrounding the clay particles gives the soil its plastic characteristics [35]. Competitive adsorption and strong polarity of water molecules are observed with the coexistence of oil and water in the contaminated loess, and part of diesel oil will be adsorbed on the surface of soil particles. The relationship between the soil particles and water molecules is weakened, for the oil molecules envelop the soil particles. The water demand for the soil particles to reach a plastic or flowing state decreases as the weakly combined water layer becomes thinner. Thus, the presence of diesel oil has led to the reduction of LL and PL.

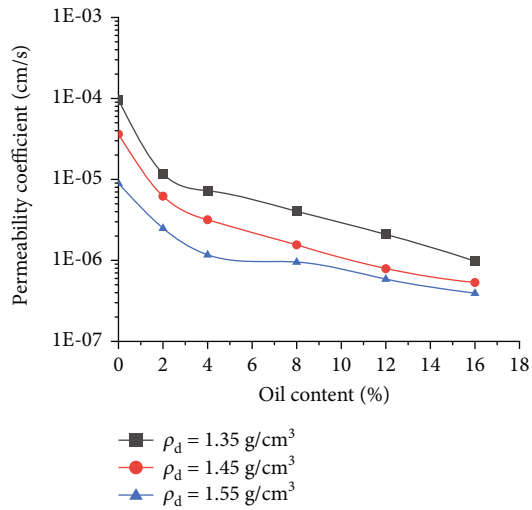

Figure 5: Permeability coefficient of diesel-contaminated loess with different oil contents.

4.2. Permeability of Contaminated Loess. The permeability of loess is a comprehensive reflection of the soil properties. When contaminated by diesel oil, the permeability of loess will change. Permeability tests were carried out to study the water physical properties of diesel-contaminated loess under different oil contents and dry densities. Figure 5 presents the relationships between the permeability coefficient of diesel-contaminated loess and oil content.

Figure 5 illustrates that the permeability coefficient of diesel-contaminated loess decreases gradually with the increase of oil content at the same dry density. When the oil content is low ($n < 4\%$), the permeability coefficient of loess contaminated by diesel oil greatly decreases, and the

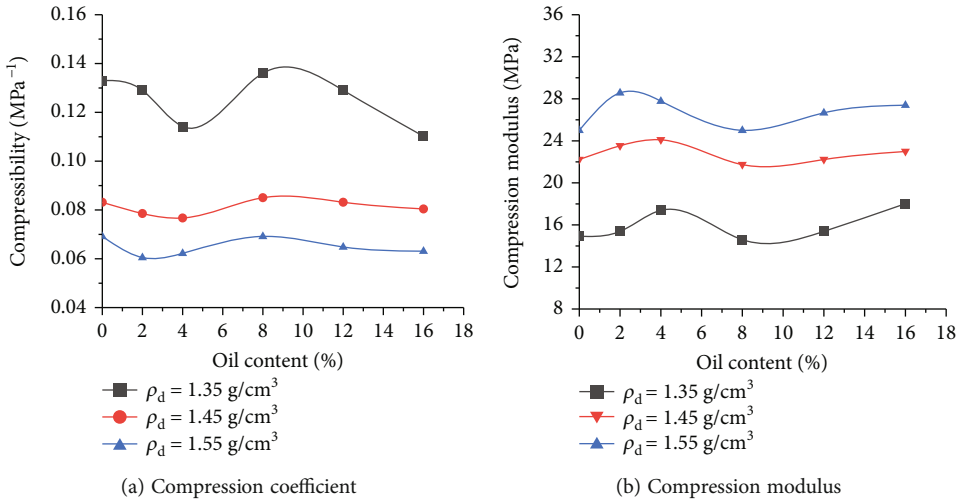

(a) Compression coefficient (b) Compression modulus

Figure 6: Compression characteristics of diesel-contaminated loess at $w = 12\%$.

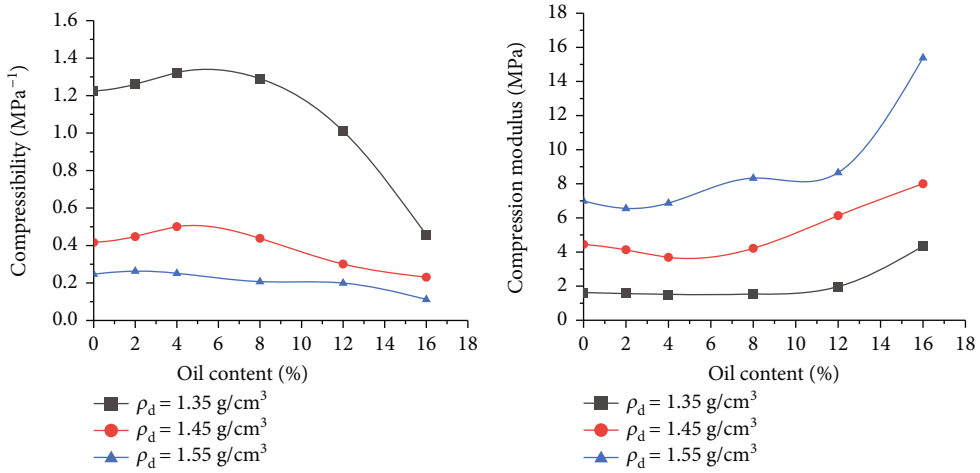

(a) Compression coefficient (b) Compression modulus

Figure 7: Compression characteristics of diesel-contaminated loess at $w = 19.6\%$.

maximum reduction is about 93% at the dry density of 1.45 g/cm^3. The decrease of the permeability coefficient of diesel-contaminated loess is relatively small at the dry density of 1.55 g/cm^3, when the oil content is more than 4%. Moreover, the permeability coefficient decreases by 6.5% when the oil content ranges from 4% to 16%. The diesel-contaminated loess is gradually compacted with the increase of dry density at the same oil content. The pores among loess particles are reduced; thus, the permeability coefficient of diesel-contaminated loess is reduced. Compared with clean loess, the permeability coefficient of diesel-contaminated loess is remarkably decreased; thus, the permeability of loess is reduced by diesel oil pollution. These findings are consistent with those obtained by Al-Aghbari et al. [13] and Abousnina et al. [14]. For loess with the same characteristics (in this research, the external environment temperature, particle composition, and chemical composition of pore water are constant), the primary factors affecting its permeability are particle size distribution, mineral composition, and porosity. Diesel oil as another fluid enters into the soil particles to fill in the pores at the same water content and dry density. The decrease of the porosity of the soil leads to the decrease of the permeability coefficient [36, 37]. When diesel oil enters the pores of soil particles, it will not flow and seep with water, and agglomeration effect will occur. Furthermore, the pores of soil particles will be blocked. Water also carries part of diesel oil in the soil to overcome the resistance of oil to pass through the pores, and oil and water two-phase seepage increases the viscosity of the seepage fluid. Therefore, the permeability coefficient sharply decreases, and it is significant that the permeability of loess is contaminated by diesel oil.

4.3. Compression Properties of Contaminated Loess. The compressibility of soil is often evaluated by the compression coefficient corresponding to the pressure range of 50, 100, 200, 400, and 800 kPa, and the deformation of the samples under each level of load is recorded. Compression modulus

refers to the ratio of the vertical additional stress and the corresponding strain of the sample in the condition of lateral restraint, which can be used to evaluate the compressibility of soil as the compression coefficient. The compression coefficient (α_v) and compression modulus (E_s) can be determined by the following equations:

$$\alpha_v = \frac{e_i - e_{i+1}}{P_{i+1} - P_i}, \quad E_s = \frac{1 + e_0}{\alpha_v}, \tag{6}$$

where e_0 is the initial void ratio of contaminated loess specimen, e_i is the void ratio of the specimen after compression and stabilization under vertical load (P_i), and e_{i+1} is the void ratio after compression and stabilization under vertical load (P_{i+1}).

4.3.1. Effect of Dry Density on Compression Properties. The compression coefficient and compression modulus of diesel-contaminated loess with different dry densities are shown in Figures 6 and 7, respectively.

As shown in Figure 6(a), at $w = 12\%$, the compression coefficient of diesel-contaminated loess decreases initially, then increases, and then gradually decreases with the increase of oil content. It fluctuates remarkably at $\rho_d = 1.35$ g/cm^3 because diesel contamination has a significant impact on the compression coefficient of loess with low dry density. The compression coefficient of diesel-contaminated loess decreases with the increase of dry density at the same oil content. Compared with clean loess, the compression coefficient of diesel-contaminated loess fluctuates up and down with the increase of oil content at the same dry density. Figure 6(b) indicates that the compression modulus of diesel-contaminated loess increases initially and then decreases with the increase of oil content ($n > 8\%$), which is contrary to the variation of the compression coefficient at the same condition.

Figure 7(a) illustrates that the compression coefficient of diesel-contaminated loess initially increases and then decreases with the increase of oil content at three dry densities. The compression coefficient of diesel-contaminated loess with different oil contents varies from 0.5 MPa^{-1} to 1.4 MPa^{-1} at $\rho_d = 1.35$ g/cm^3, which refers to the high compression of contaminated loess because of the effect of diesel oil. Compared with clean loess, the compression coefficient of diesel-contaminated loess is basically greater, when the oil content is less than 8%. However, it is gradually smaller than that of clean loess when the oil content exceeds 8%. As shown in Figure 7(b), it can be revealed that the compression modulus of diesel oil-contaminated loess decreases initially and then increases with the increase of oil content at the same density. Under the condition of $\rho_d = 1.35$ g/cm^3, the compression modulus of loess increases from 6.9 MPa to 15 MPa, an increase of 117%. However, the changes of compression modulus are relatively gentle at $\rho_d = 1.45$ g/cm^3 and 1.55 g/cm^3. Thus, this result is contrary to the change law of compression coefficient of diesel-contaminated loess, which is in accordance with the actual situation.

4.3.2. Effect of Water Content on Compression Properties. Based on the analysis and summary of the abovementioned test results, a certain relationship can be observed between the compression characteristics of diesel-contaminated loess and water contents of diesel-contaminated loess. At $w = 12\%$ and $w = 19.6\%$, the curves of compression coefficient and compression modulus of diesel-contaminated loess with the increase of oil contents are plotted in Figure 8.

As shown in Figure 8, the compression characteristics of diesel-contaminated loess have different change laws under different water contents. At $w = 12\%$, the compression coefficient of contaminated loess decreases initially, then increases, and then decreases with the increase of oil content (0 to 16%). It all reaches the minimum when the oil content is close to 4% and reaches the maximum value when the oil content approaches 9% at three different dry densities. However, the compression coefficient of contaminated loess increases initially and then decreases with the increase of oil content at $w = 19.6\%$, and it all reaches the maximum value when the oil content reaches 5% at different dry densities.

It also can be seen that the oil content increases from 0% to 8%, and the variation of the compression coefficient of diesel-contaminated loess is opposite at two different water contents. When the oil content is more than 8%, it has the same change laws, showing a decrease with the increase of oil content. Compared with the diesel-contaminated loess with $w = 19.6\%$, the compression coefficient of diesel-contaminated loess with $w = 12\%$ slightly changes, which is basically a straight line with the increase of oil content. Therefore, when the water content of diesel-contaminated loess is large, the change of compression coefficient is evident. By contrast, when the water content is low, and the dry density is large, the change of compression coefficient is not evident. However, with the increase of oil content, both change laws of compression modulus with two different water contents are opposite to those of the compression coefficient of diesel-contaminated loess at the same dry density.

4.4. Compressive Strength Characteristics of Diesel-Contaminated Loess

4.4.1. Effect of Dry Density on Unconfined Compressive Strength. The unconfined compressive strength test of contaminated loess with oil content ranging from 0 to 16% was carried out, and the test results were analyzed. The relationships between the unconfined compressive strength (q_u) of diesel-contaminated loess and oil content are shown in Figures 9 and 10 at three different dry densities, respectively.

Figure 9 shows that diesel-contaminated loess with the same oil content has a remarkable unconfined compressive strength (q_u) when the dry density is high at $w = 12\%$. The general law of unconfined compressive strength changing with the oil content of diesel-contaminated loess is that it reaches the maximum value when oil content approaches

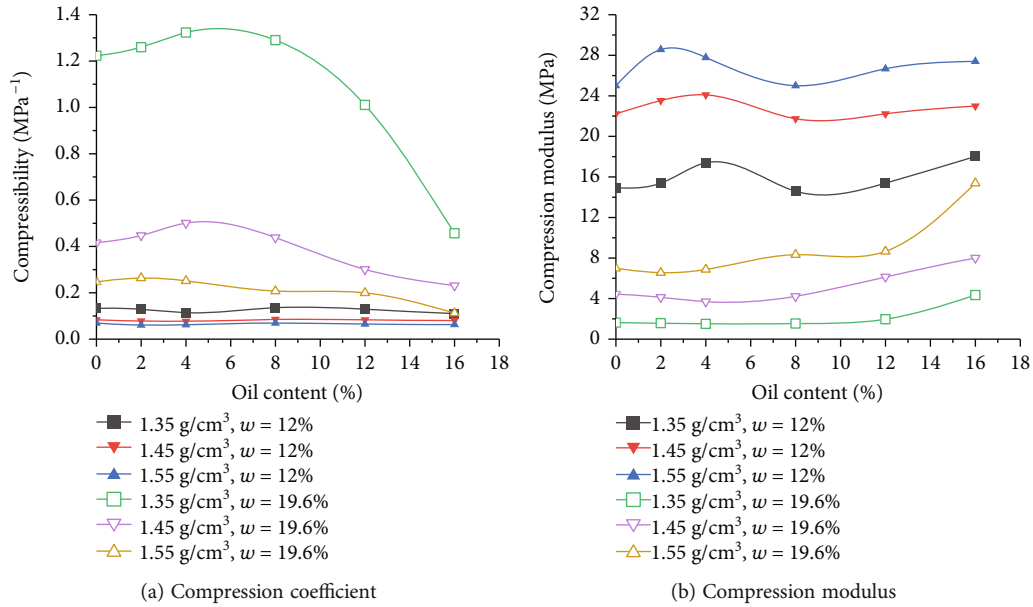

Figure 8: Comparison of compression characteristics of diesel-contaminated loess with different water contents.

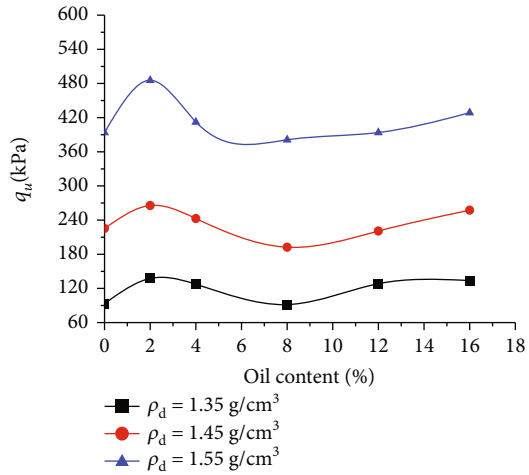

Figure 9: Unconfined compressive strength of diesel-contaminated loess at $w = 12\%$.

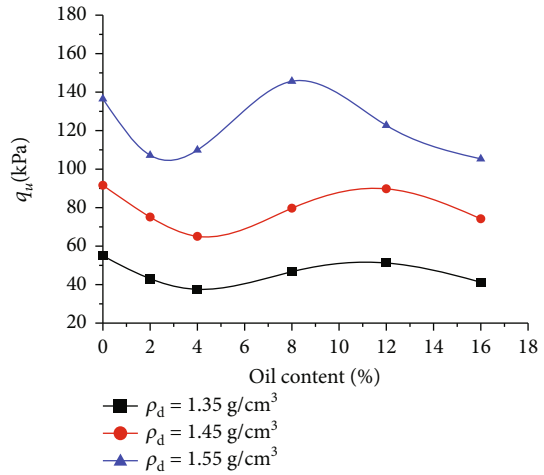

Figure 10: Unconfined compressive strength of diesel-contaminated loess at $w = 19.6\%$.

2%. Considering that diesel oil has a certain viscosity, and the oil content of diesel-contaminated loess is low, its viscosity is greater than the viscosity of the pore water between the soil particles, which increases the viscosity of the loess particles. With the increase of oil content, unconfined compressive strength decreases initially. When the oil content is more than 8%, it increases slowly. Given the viscosity of diesel oil, the contact between soil particles is close, thereby forming a pseudoviscosity [38], and diesel oil is the primary factor of the compressive strength of loess. Compared with clean loess, the unconfined compressive strength of contaminated loess is greater, except for the contaminated loess with 8% oil content. The findings of these tests are similar to the results of the compression tests. Given the increase of oil content, the variation of the compression modulus and unconfined compressive strength of diesel oil-contaminated loess is consistent at the same dry density.

As shown in Figure 10, the higher the dry density of diesel-contaminated loess with the same density is, the greater the unconfined compressive strength (q_u) will be at $w = 19.6\%$. The change laws of unconfined compressive strength of contaminated loess decrease initially, then increase, and then reduce gradually with the increase of oil content at three different dry densities. When oil content is 4%, the unconfined compressive strength of contaminated loess reaches the minimum value at $\rho_d = 1.35\,g/cm^3$ and $1.45\,g/cm^3$, and it shows a minimum value of contaminated loess with the oil content approaching 3% ($\rho_d = 1.55\,g/cm^3$), while it reaches the peak point when the oil content approaches 8%. Compared with the clean loess, the

(a) 2% oil content, $\rho_d = 1.55\,g/cm^3$ (b) 12% oil content, $\rho_d = 1.55\,g/cm^3$

Figure 11: Typical failure patterns of diesel-contaminated loess at $w = 12\%$.

(a) 2% oil content, $\rho_d = 1.55\,g/cm^3$ (b) 12% oil content, $\rho_d = 1.55\,g/cm^3$

Figure 12: Typical failure patterns of diesel-contaminated loess at $w = 19.6\%$.

unconfined compressive strength of the diesel-contaminated loess is basically lower with increasing oil contents at $\rho_d = 1.35\,g/cm^3$, $1.45\,g/cm^3$, and $\rho_d = 1.55\,g/cm^3$. When the oil content ranges from 0 to 12%, the change law of the compression modulus and unconfined compressive strength of contaminated loess in compression tests is consistent at the same dry density.

4.4.2. Effect of Water on Unconfined Compressive Strength Characteristics. Unconfined compressive strength tests were carried out on contaminated samples with different water contents ($w = 12\%$, 19.6%); the failure patterns of diesel-contaminated loess were different. The typical failure patterns of diesel-contaminated loess under two different water contents ($w = 12\%$, 19.6%) are shown in Figures 11 and 12, respectively.

By comparing Figures 11 and 12, the failure of diesel-contaminated loess samples occurs rapidly at $w = 12\%$. After the specimen compressed, small oblique cracks without penetration begin to appear and expand to depth. At the same time, a small amount of vertical microcracks occur at the end of the sample, and then, the stress increases, the cracks of the sample quickly penetrate obliquely, and most of the samples are suddenly damaged and cracked into multiple pieces. As shown in the literatures [39–41], failure modes had certain regularity. The fracturing and damage forms of samples show different characteristics under different test conditions [42, 43]. Compared with the diesel oil-contaminated loess sample ($w = 12\%$), the crack penetration of the sample is relatively slow at $w = 19.6$. At first, the sample appears as small cracks and then gradually expands. The oblique cracks gradually penetrate to form a rupture surface, and the sample is damaged.

Based on the analysis of the unconfined compressive strength test results of diesel-contaminated loess at two different water contents, the unconfined compressive strength (q_u) curves of diesel-contaminated loess with different oil contents and dry densities are shown in Figure 13.

Although the pollution degree of the loess sample is the same at the two different water contents, the air-dried loess

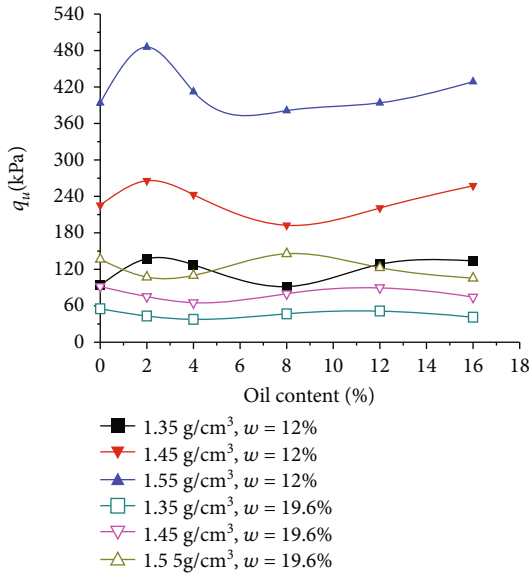

Figure 13: Comparison of the unconfined compressive strength of diesel-contaminated loess with different water contents.

is first combined with water to form certain water contents (w = 12%, 19.6%) and then added with diesel oil to prepare contaminated loess samples. In Figure 13, the unconfined compressive strength initially shows an increasing trend, then decreasing, and then increasing with the increase of oil content (w = 12%). When oil content is low, diesel oil fills in the pores of soil particles, and its viscosity is greater than that of the sample that fills in the pores with water; therefore, diesel oil increases the viscosity of soil particles [17]. Therefore, as the cementing ability of diesel-contaminated loess strengthens, the unconfined compressive strength increases. When the oil content of diesel-contaminated loess continues to increase, the pores of soil particles will be gradually filled. Moreover, the viscosity of diesel oil is less than its own lubrication effect, and the relative sliding between soil particles becomes easy, which decreases the unconfined compressive strength of diesel oil-contaminated loess.

Given the effects of water contents, the unconfined compressive strength of loess is different under the same conditions. Compared with the contaminated loess at w = 12%, the unconfined compressive strength decreases with the increase of oil content at w = 19.6%. The loess initially combines with water, and the double-layer water is formed between the soil particles. The water molecules close to the surface of the soil particles are affected by the electric field force [44]. Moreover, it forms strong bound water on the surface of the soil particles, and the arrangement of the water molecules is approximately fixed. The loess gradually loses the liquid characteristics and approximates the solid characteristics [45]. Therefore, the compressive strength of contaminated loess at w = 12% is relatively higher than that at w = 19.6%. When the oil content is at a low level, the unconfined compressive strength fluctuates remarkably with the increase of oil content. When the water content of diesel-contaminated loess is less, the change of compressive strength is evident at the same condition. However, with high water content and low dry density, the variation of compressive strength is not evident. Therefore, underthe two different water contents, the change law of the unconfined compressive strength of contaminated loess with the increase of oil content is opposite at the same dry density.

5. Conclusions

In order to better evaluate the physical and mechanical properties of loess contaminated by diesel oil, a series of laboratory tests were performed under different test conditions. The conclusions are as follows:

(1) Diesel contamination has changed the physical and mechanical properties of loess, with Atterberg limits and permeability of loess affected by oil content. Compared with clean loess, a decrease is found in liquid limits (LL), plastic limits (PL), plasticity index (PI), and permeability coefficient of diesel-contaminated loess with the increase of oil content

(2) The variation of the compression characteristics of loess caused by diesel leakage pollution is complex. The compression coefficient of diesel-contaminated loess decreases with the increase of dry density. When the dry density is large, and the water content is low, the change of compression coefficient is not evident, but the change law of compression modulus is opposite

(3) The higher the dry density of oil-contaminated loess is, the greater its compressive strength will be at the same oil content. The water content of contaminated loess also has a great effect on its compressive strength characteristics. Under the two different water contents (w = 12%, 19.6%), the change law of the unconfined compressive strength of contaminated loess with the increase of oil content is opposite at the same dry density

(4) The findings of unconfined compressive strength tests are similar to the results of the compression tests. With the increase of oil content, the change laws of the compression modulus and unconfined compressive strength of diesel oil-contaminated loess are similar under the same condition

Data Availability

All the data used to support the findings of this study are included within the article.

Conflicts of Interest

The authors declare that there is no conflict of interest.

Acknowledgments

This study was supported by the National Natural Science Foundation of China (No. 41877278), the China Geological

Survey (No. DD20190268), and the Key R&D program of Shaanxi Province (No. 2020ZDLGY07-03).

References

[1] H. Soltani-Jigheh, H. V. Molamahmood, T. Ebadi, and A. A. Soorki, "Effect of oil-degrading bacteria on geotechnical properties of crude oil-contaminated sand," *Environmental & Engineering Geoscience*, vol. 24, no. 3, pp. 333–341, 2018.

[2] Y. Li and L. Jiang, "Comparison of the crude oil removal effects of different surfactants in electrokinetic remediation of low-permeability soil," *Journal of Environmental Chemical Engineering*, vol. 9, no. 4, article 105190, 2021.

[3] A. Mohammadi, T. Ebadi, and M. R. Boroomand, "Physical modelling of axial compressive bearing capacity of instrumented piles in oil-contaminated sandy soil," *Iranian Journal of Science and Technology, Transactions of Civil Engineering*, vol. 44, no. 2, pp. 695–714, 2020.

[4] A. R. Estabragh, I. Beytolahpour, M. Moradi, and A. A. Javadi, "Consolidation behavior of two fine-grained soils contaminated by glycerol and ethanol," *Engineering Geology*, vol. 178, pp. 102–108, 2014.

[5] R. M. Abousnina, A. Manalo, W. Lokuge, and Z. Zhang, "Effects of light crude oil contamination on the physical and mechanical properties of geopolymer cement mortar," *Cement and Concrete Composites*, vol. 90, pp. 136–149, 2018.

[6] C. C. Huang, "Effects of restraining conditions on the bearing capacity of footings near slopes," *Soils and Foundation*, vol. 59, no. 1, pp. 1–12, 2019.

[7] R. C. Randolph, J. T. Hardy, S. W. Fowler, R. G. Andrew, and H. P. Walter, "Toxicity and persistence of nearshore sediment contamination following the 1991 Gulf War," *Environment International*, vol. 24, no. 1-2, pp. 33–42, 1998.

[8] H. A. Alsanad, W. K. Eid, and N. F. Ismael, "Geotechnical properties of oil-contaminated Kuwaiti sand," *Journal of Geotechnical Engineering*, vol. 121, no. 5, pp. 407–412, 1995.

[9] H. A. Alsanad and N. F. Ismael, "Aging effects on oil-contaminated Kuwaiti sand," *Journal of Geotechnical & Geoenvironmental Engineering*, vol. 123, no. 3, pp. 290–293, 1997.

[10] A. M. A. Nasr, "Experimental and theoretical studies for the behavior of strip footing on oil-contaminated sand," *Journal of Geotechnical and Geoenvironmental Engineering*, vol. 135, no. 12, pp. 1814–1822, 2009.

[11] B. P. Chaplin, G. N. Delin, R. J. Baker, and M. A. Lahvis, "Long-term evolution of biodegradation and volatilization rates in a crude oil-contaminated aquifer," *Bioremediation Journal*, vol. 6, no. 3, pp. 237–255, 2002.

[12] S. A. Aiban, "The effect of temperature on the engineering properties of oil-contaminated sands," *Environment International*, vol. 24, no. 1-2, pp. 153–161, 1998.

[13] M. Al-Aghbari, R. Dutta, and Y. Mohamedzeini, "Effect of diesel and gasoline on the properties of sands-a comparative study," *International Journal of Geotechnical Engineering*, vol. 5, no. 1, pp. 61–68, 2011.

[14] R. M. Abousnina, A. Manalo, J. Shiau, and W. Lokuge, "Effects of light crude oil contamination on the physical and mechanical properties of fine sand," *Soil & Sediment Contamination an International Journal*, vol. 24, no. 8, pp. 833–845, 2015.

[15] M. Ostovar, R. Ghiassi, M. J. Ehdizadeh, and N. Shariatmadari, "Effects of crude oil on geotechnical specification of sandy soils," *Soil & Sediment Contamination*, vol. 30, no. 1, pp. 58–73, 2021.

[16] G. Fazeli, S. Lotfollahi, P. Bakhtiari, and F. Farrokhi, "Bearing capacity and geotechnical properties of a sandy soil substrate contaminated with oil derivatives (diesel fuel and kerosene)," *Quarterly Journal of Engineering Geology and Hydrogeology*, vol. 54, no. 4, article qjegh2020-134, 2021.

[17] M. Khamehchiyan, A. Hossein Charkhabi, and M. Tajik, "Effects of crude oil contamination on geotechnical properties of clayey and sandy soils," *Engineering Geology*, vol. 89, no. 3-4, pp. 220–229, 2007.

[18] Z. A. Rahman, U. Hamzah, M. R. Taha, N. S. Ithnain, and N. Ahmad, "Influence of oil contamination on geotechnical properties of basaltic residual soil," *American Journal of Applied Sciences*, vol. 7, no. 7, pp. 954–961, 2010.

[19] T. Zheng, J. Yang, J. Liu, and L. Tong, "Compaction properties of oil contaminated soil," *Hydrogeology and Engineering Geology*, vol. 37, no. 3, pp. 102–106, 2010.

[20] T. Zheng, J. Yang, Y. Li, and J. Liu, "Experimental study on engineering properties of diesel contaminated soil," *Geotechnical Investigation & Surveying*, vol. 1, pp. 1–4, 2013.

[21] H. Safehian, A. M. Rajabi, and H. Ghasemzadeh, "Effect of diesel-contamination on geotechnical properties of illite soil," *Engineering Geology*, vol. 241, pp. 55–63, 2018.

[22] E. Khosravi, H. Ghasemzadeh, and M. R. Sabour, "Geotechnical properties of gas oil-contaminated kaolinite," *Engineering Geology*, vol. 166, pp. 11–16, 2013.

[23] S. Xie, M. Li, H. Du, D. Li, and J. Zhang, "Influence of environment temperature on strength and deformation of saline soil in inshore contaminated by petroleum," *Journal of Engineering Geology*, vol. 24, no. 4, pp. 616–621, 2016.

[24] M. Li, C. Wang, H. Du, and J. Zhang, "Mechanical properties of oil contaminated saline soil solidified with lime and fly ash," *Chinese Journal of Rock Mechanics and Engineering*, vol. 37, no. s1, pp. 3578–3586, 2017.

[25] K. Iqbal, C. S. Xu, H. Nasir, and M. Alam, "Effect of used motor oil and bitumen as additive on the permeability and mechanical properties of low plastic soil," *Advances in Materials Science and Engineering*, vol. 2021, no. 1, Article ID 1360197, 2020.

[26] K. Mohammad and E. Taghi, "The effect of oil contamination on the geotechnical properties of fine-grained soils," *Soil & Sediment Contamination An International Journal*, vol. 21, no. 5, pp. 655–671, 2012.

[27] P. Hou, X. Liang, F. Gao, J. B. Dong, J. He, and Y. Xue, "Quantitative visualization and characteristics of gas flow in 3D pore-fracture system of tight rock based on lattice Boltzmann simulation," *Journal of Natural Gas Science and Engineering*, vol. 89, no. 4, article 103867, 2021.

[28] P. Hou, X. Liang, Y. Zhang, J. He, F. Gao, and J. Liu, "3D multi-scale reconstruction of fractured shale and influence of fracture morphology on shale gas flow," *Natural Resources Research*, vol. 30, no. 3, pp. 2463–2481, 2021.

[29] L. Qin, P. Wang, S. G. Li et al., "Gas adsorption capacity changes in coals of different ranks after liquid nitrogen freezing," *Fuel*, vol. 292, article 120404, 2021.

[30] X. Liang, P. Hou, Y. Xue, X. J. Yang, F. Gao, and J. Liu, "A fractal perspective on fracture initiation and propagation of reservoir rocks under water and nitrogen fracturing," *Fractals-Complex Geom, Patterns and Scaling in nature and Society*, vol. 29, no. 7, article 2150189, 2021.

[31] National Standards of the PRC, "Standard for geotechnical testing method GB/T," China Planning Press, 2019.

[32] C. Liang, X. Zheng, J. Zhang, and F. Yue, "Testing of water content in oil-contaminated porous medium," *Journal of Jilin University*, vol. 41, no. 3, pp. 826–830, 2011.

[33] L. Tong, W. Chen, X. Zheng, and M. Li, "Capillary rise of water in diesel oil contaminated soils," *Journal of Irrigation and Drainage*, vol. 30, no. 6, pp. 131–134, 2011.

[34] M. Kermani and T. Ebadi, "The effect of oil contamination on the geotechnical properties of fine-grained soils," *Soil & sediment contamination*, vol. 21, no. 5, pp. 655–671, 2012.

[35] B. M. Das, *Advanced Soil Mechanics*, CRC press, Taylor & Francis Group, 4th edition, 2014.

[36] H. H. Becher, "Soil physical properties of subsoils contaminated with light nonaqueous phase liquids (INAPLs)," *Journal of Plant Nutrition and Soil Science*, vol. 164, no. 5, pp. 579–584, 2001.

[37] M. Ahmadi, T. Ebadi, and R. Maknoon, "Effects of crude oil contamination on geotechnical properties of sand-kaolinite mixtures," *Engineering Geology*, vol. 283, article 106021, 2021.

[38] L. Tong, *Study on water-physical and mechanical properties of oil-contaminated soils*, Ocean University of China, 2008.

[39] T. L. Han, Z. H. Li, and Y. S. Chen, "Sulfate attack induced dry-wet failure modes and a constitutive model for mortar specimens with a single intermittent fracture," *International Journal of Geomechanics*, vol. 21, no. 2, article 04020249, 2021.

[40] T. L. Han, J. P. Shi, Y. S. Chen, and Z. H. Li, "Quantifying microstructural damage of sandstone after hydrochemical corrosion," *International Journal of Geomechanics*, vol. 18, no. 10, article 04018121, 2018.

[41] T. L. Han, X. F. Wang, D. F. Li, D. W. Li, N. X. Han, and F. Xing, "Damage and degradation mechanism for single intermittent cracked mortar specimens under a combination of chemical solutions and dry-wet cycles," *Construction and Building Materials*, vol. 213, pp. 567–581, 2019.

[42] L. Qin, C. Ma, S. G. Li et al., "Mechanical damage mechanism of frozen coal subjected to liquid nitrogen freezing," *Fuel*, vol. 309, article 122124, 2022.

[43] T. L. Han, J. P. Shi, and X. S. Cao, "Fracturing and damage to sandstone under coupling effects of chemical corrosion and freeze-thaw cycles," *Rock Mechanics and Rock Engineering*, vol. 49, no. 11, pp. 4245–4255, 2016.

[44] X. M. Duan, "Mechanical effects of solid water on the particle skeleton of soil: mechanism analysis," *Geofluids*, vol. 2021, no. - article 9969023, 2021.

[45] Y. Zhang, T. Chen, Z. Wang, and Y. Zhang, "An equivalent method for calculating the seepage coefficient of clay based on solidified micro-bound water," *Chinese Journal of Rock Mechanics and Engineering*, vol. 37, no. 4, pp. 1004–1010, 2018.